International Journal of Thermophysics, Vol. 17, No. 4, 1996

Vapor–Liquid Equilibria of Binary Mixtures Containing Methane, Ethane, and Carbon Dioxide from Molecular Simulation

J. Vrabec[1] and J. Fischer[2, 3]

Received September 25, 1995

The $NpT+$ test particle method is used in order to predict vapor–liquid equilibria of the mixtures methane + ethane, methane + carbon dioxide, and carbon dioxide + ethane by molecular simulations. The pure-component molecular models were fitted to the experimental vapor pressures and saturated liquid densities in previous papers, which used the same simulation method for the determination of the phase equilibria. For each binary mixture the two unlike interaction parameters were determined from one experimental excess volume and one excess enthalpy. Based on these molecular models the vapor–liquid phase equilibria were calculated for each mixture at three temperatures. Comparison of the pressure-composition data with experimental results shows the high predictive power of this molecular based procedure. This statement is confirmed by additional comparisons of the pressure-composition diagrams and the pressure-density diagrams with results from equations of state.

KEY WORDS: biogas; molecular interactions; molecular simulations; natural gas; vapor–liquid equilibria.

1. INTRODUCTION

The calculation of thermodynamic properties from molecular models is a long-lasting aim and has been considerably facilitated by the use of computer simulations. A topic of special interest also with respect to practical applications is the easy and accurate simulation of phase equilibria. In that field, recently, remarkable progress was made. One frequently used method

[1] Institut für Thermo- und Fluiddynamik, Ruhr-Universität, D-44780 Bochum, Germany.
[2] Institut für Land-, Umwelt- und Energietechnik, Universität für Bodenkultur, A-1190 Wien, Austria.
[3] To whom correspondence should be addressed.

840/17/4-11

is the Gibbs ensemble, which was introduced by Panagiotopoulos [1] and applied to pure fluids and mixtures [2–5]. Alternatively, the $NpT+$ test particle method was proposed [6] and first applied to pure fluids [7–9], including carbon dioxide [10]. Recently, the method was extended to mixtures and applied to argon + methane [11] and a series of Lennard–Jones mixtures [12]. The purpose of the present paper is to demonstrate that the $NpT+$ test particle method also works well for nonspherical and polar molecules. In particular, we want to consider three key mixtures, namely, methane + ethane, methane + carbon dioxide, and carbon dioxide + ethane. The first and third of these mixtures are of great technical interest in energy and petroleum engeneering; the second mixture is known as biogas.

The calculation of thermodynamic properties by statistical mechanics requires models for the intermolecular potentials between the like and the unlike molecules. For the determination of the pure-component interactions, an established procedure assumes a physically reasonable model for the interaction with few adjustable parameters to be fitted to the saturated properties of the liquid. Such effective intermolecular potentials are available for the substances under present consideration [10, 13, 14]. In addition, it was suggested earlier [15] to determine the unlike interaction parameters by fitting to one experimental excess volume and one excess enthalpy. This work has to be done here for the three unlike interactions of the binary mixtures.

The paper is organized such that we give an outline of the method in the next section. Then the molecular models are given for the pure components and determined for the unlike interactions. Finally, vapor–liquid equilibria are presented for each system at three temperatures and compared to experimental data and to equation of state (EOS) results.

2. OUTLINE OF THE METHOD

We consider a binary mixture consisting of components A and B ($i = A, B$) with a given complete set of like and unlike intermolecular potentials between the particles. The basic idea of the $NpT+$ test particle method for the determination of vapor–liquid phase equilibria of binary mixtures is to construct at a prescribed temperature T and a prescribed liquid composition x, the chemical potentials as functions of the pressure $\mu_i^l(p)$, and in the vapor as functions of the pressure and the vapor composition $\mu_i^v(p, y_A)$ by simulations. Because of the prescription of the pressure it is essential to use the isobaric isothermal NpT ensemble, but it should be mentioned that it does not matter whether molecular dynamics or Monte Carlo simulation technique is used. When the construction is done, the vapor pressure p_σ and the vapor composition in equilibrium y can be

calculated by using the equality of the chemical potentials in the two phases

$$\mu_{i\sigma} = \mu_i^{\mathrm{l}}(p_\sigma) = \mu_i^{\mathrm{v}}(p_\sigma, y), \qquad (i = A, B) \tag{1}$$

where $\mu_{i\sigma}$ denotes the chemical potential of component i at phase equilibrium.

Now let us start with the equations which shall be evaluated by simulations at prescribed values of the temperature T, the pressure p, and the composition x. For the chemical potentials we apply Widom's test particle method [16], according to which

$$\mu_i = \mu^{\mathrm{id}}(T) + kT \ln x_i - kT \ln \langle V \exp\{-\beta\psi_i\} \rangle / N \tag{2}$$

where ψ_i denotes the potential energy of the test particle of the species i, V the instantaneous volume and the brackets averaging in the NpT ensemble; $\mu^{\mathrm{id}}(T)$ is the merely temperature dependent part of the chemical potential. Widom's test particle method yields also the partial molar volumes v_i by the average [17, 18]

$$v_i = \frac{\langle V^2 \exp\{-\beta\psi_i\} \rangle}{\langle V \exp\{-\beta\psi_i\} \rangle} - \langle V \rangle \tag{3}$$

From a NpT simulation we obtain directly the density ρ and the enthalpy h. Moreover, we calculate the isothermal compressibility β_T as

$$\beta_T = \frac{1}{kT} \frac{1}{\langle V \rangle} [\langle V^2 \rangle - \langle V \rangle^2] \tag{4}$$

and the derivative of the enthalpy with respect to the pressure at constant temperature and constant composition $(\partial h/\partial p)_{T,x}$ as

$$\left(\frac{\partial h}{\partial p}\right)_{T,x} = \frac{1}{N} \left\{ -\frac{1}{kT} [\langle HV \rangle - \langle H \rangle \langle V \rangle] + \langle V \rangle \right\} \tag{5}$$

where H denotes the instantaneous enthalpy. The complete set of thermodynamic quantities that we have to calculate from every simulation at prescribed T, x, and p is ρ, h, β_T, $(\partial h/\partial p)_{T,x}$, μ_i, and v_i.

The next item is the construction of the functions for the chemical potentals needed for Eq. (1). In order to obtain $\mu_i^{\mathrm{l}}(p)$, the performance of one simulation at an arbitrary chosen pressure p_0^{l} is sufficient, where p_0^{l} should be not too far from the unknown vapor pressure p_σ. At low

temperatures $p_0^l = 0$ can be taken as a guess. Having fixed T, x, and p_0^l, and keeping in mind that

$$\left(\frac{\partial \mu_i}{\partial p}\right)_{T,x} = v_i \tag{6}$$

we can approximate with sufficient accuracy $\mu_i^l(p)$ by a first-order Taylor expansion from this single-liquid simulation,

$$\mu_i^l(p) \approx \mu_{i0}^l + v_i^l(p - p_0^l) \tag{7}$$

For the vapor phase some more effort has to be done. The full chemical potentials split into the ideal and residual parts

$$\mu_i = \mu_i^{res} + kT \ln \frac{p}{kT} + kT \ln y_i + \mu^{id}(T) \tag{8}$$

with

$$\mu_i^{res} = \mu_i(T, p, y_i) - \mu_i^{id}(T, p, y_i)$$

The μ_i typically show in the vapor a logarithmic dependence on the pressure and composition. This prevents an accurate approximation by a first-order Taylor expansion. Therefore we expand, starting from an arbitrary chosen pair of p_0^v and y_{A0}, only the residual part of the chemical potentials, treating the ideal parts analytically

$$\mu_i^v(p, y_A) \approx \mu_{i0}^v + \left(\frac{\partial \mu_i^{v,\,res}}{\partial p}\right)_{T,x} (p - p_0^v) + kT \ln \left(\frac{p}{p_0^v}\right) + \left(\frac{\partial \mu_i^{res}}{\partial y_A}\right)_{T,p} (y_A - y_{A0}) + kT \ln \left(\frac{y_i}{y_{i0}}\right) \tag{9}$$

The derivatives of the residual chemical potentials with respect to the pressure are given from an evaluation of Eq. (3) as

$$\left(\frac{\mu_i^{v,\,res}}{\partial p}\right)_{T,x} = v_i^v - v^{id} = v_i^v - \frac{kT}{p} \tag{10}$$

In order to obtain the dependence of the residual chemical potentials due to composition change at constant temperature and constant pressure, a second simulation in the vapor phase at the same temperature and

pressure, but at a different vapor composition y_{A1}, has to be performed. The needed derivatives are then approximated by difference ratios

$$\left(\frac{\partial \mu_i^{\mathrm{v,\,res}}}{\partial y_A}\right)_{T,p} \approx \left(\frac{\mu_{i1}^{\mathrm{v,\,res}} - \mu_{i0}^{\mathrm{v,\,res}}}{y_{A1} - y_{A0}}\right)_{T,p} = \left(\frac{\Delta \mu_i^{\mathrm{v,\,res}}}{\Delta y_A}\right)_{T,p} \tag{11}$$

so that our working equation for the vapor writes as

$$\mu_i^{\mathrm{v}}(p, y_A) \approx \mu_{i0}^{\mathrm{v}} + \left(v_i^{\mathrm{v}} - \frac{kT}{p}\right)(p - p_0^{\mathrm{v}}) + kT \ln\left(\frac{p}{p_0^{\mathrm{v}}}\right) + \left(\frac{\Delta \mu_i^{\mathrm{v,\,res}}}{\Delta y_A}\right)_{T,p} (y_A - y_{A0}) + kT \ln\left(\frac{y_i}{y_{i0}}\right) \tag{12}$$

Finally, by equating Eqs. (7) and (12), we obtain the vapor pressure and vapor composition for the prescribed values of temperature and liquid composition at the coexistence point.

The bubble density ρ', the dew density ρ'', the bubble enthalpy h', and the dew enthalpy h'' are also calculated with first-order Taylor series, by inserting the vapor pressure and vapor composition,

$$\rho' \approx \rho_0^{\mathrm{l}} + \beta_T^{\mathrm{l}} \rho_0^{\mathrm{l}} (p_\sigma - p_0^{\mathrm{l}}) \tag{13}$$

$$\rho'' \approx \rho_0^{\mathrm{v}} + \beta_T^{\mathrm{v}} \rho_0^{\mathrm{v}} (p_\sigma - p_0^{\mathrm{v}}) + \left(\frac{\partial \rho^{\mathrm{v}}}{\partial y_A}\right)_{T,p} (y - y_{A0}) \tag{14}$$

$$h' \approx h_0^{\mathrm{l}} + \left(\frac{\partial h^{\mathrm{l}}}{\partial p}\right)_{T,x} (p_\sigma - p_0^{\mathrm{l}}) \tag{15}$$

$$h'' \approx h_0^{\mathrm{v}} + \left(\frac{\partial h^{\mathrm{v}}}{\partial p}\right)_{T,y} (p_\sigma - p_0^{\mathrm{v}}) + \left(\frac{\partial h^{\mathrm{v}}}{\partial y_A}\right)_{T,p} (y - y_{A0}) \tag{16}$$

The coefficients β_T and $(\partial h/\partial p)_{T,x}$ are obtained with the fluctuation formulae, Eqs. (4) and (5). The derivatives of the density and enthalpy with respect to the vapor composition are again approximated as difference ratios of the two vapor simulation results.

In general, the $NpT+$ test particle method for binary mixtures requires three simulation runs, one in the liquid and two for the vapor. But in most cases the density of the considered vapor is low, so that simple EOS

(e.g., virial expansion, perturbed virial expansion) can be used instead of Eq. (12). This reduces the number of simulation runs to one per coexistence point.

3. MOLECULAR MODELS

The binary mixtures investigated here are the three possible combinations of methane, ethane, and carbon dioxide. For all of these pure substances reliable molecular models are available. Methane is modeled as a one-center Lennard–Jones fluid [13], ethane as a two-center Lennard–Jones fluid [14], and carbon dioxide as a two-center Lennard–Jones plus point quadrupole fluid [10], cf. Table I. The item of this paper is the VLE of mixtures, but it is important to know about the behavior of the pure-fluid models in comparison to the real fluids. Deviation plots for the vapor pressure and the bubble density are given in the literature for methane in Ref. 11 and for ethane in Ref. 14, but not for carbon dioxide. Therefore we performed simulations to calculate the VLE of the carbon dioxide model at 12 temperatures; the deviation plots are shown in Fig. 1. We can observe the agreement of the vapor pressure mostly within the statistical uncertainties. The bubble density agrees in the lower and middle temperature range well, but approaching the critical point, the model shows too high bubble densities. This fits into the general picture for all models referred here, which is caused by a somewhat too high critical temperature, resulting in general from simulations due to finite size effects.

Having fixed the models for the like potential parameters, it is necessary to determine the unlike interactions for all three mixtures. They are usually expressed through the unlike interaction parameters η and ξ and the like potential parameters as

$$\sigma_{AB} = \eta \tfrac{1}{2}(\sigma_A + \sigma_B) \tag{17}$$

and

$$\varepsilon_{AB} = \xi \sqrt{\varepsilon_A \varepsilon_B} \tag{18}$$

If $\eta = \xi = 1$, Eqs. (17) and (18) are the Lorentz–Berthelot (LB) combining rules. We will evaluate here η and ξ for the three mixtures in the same way as Möller et al. [15], by fitting the calculated v^E and h^E values to experimental data. The procedure in detail is as follows: assuming in a run the LB combining rules we determine the coresponding v_{LB} and h_{LB} values. From the same simulation run the derivatives of v^E and h^E with respect to η and ξ, namely, $(\partial v^E/\partial \eta)$, $(\partial v^E/\partial \xi)$, $(\partial h^E/\partial \eta)$, and $(\partial h^E/\partial \xi)$ are calculated by fluctuation formulae [19]. With the help of two additional simulations at the same temperature and pressure for both pure

Table I. Parameters for the Molecular Interactions for Methane Modeled as a Lennard–Jones Fluid [13], for Ethane as a Two-Center Lennard–Jones Fluid with the Elongation $L^* = l/\sigma$ [14], and for Carbon Dioxide as a Two-Center Lennard–Jones Plus Point Quadrupole Fluid with $Q^{*2} = Q^2/\varepsilon\sigma^5$ [10]

Substance	σ (Å)	ε/k (K)	L^*	Q^{*2}
Methane	3.7275	148.99	—	—
Ethane	3.5000	135.57	0.67	—
Carbon dioxide	3.0354	125.317	0.699	3.0255

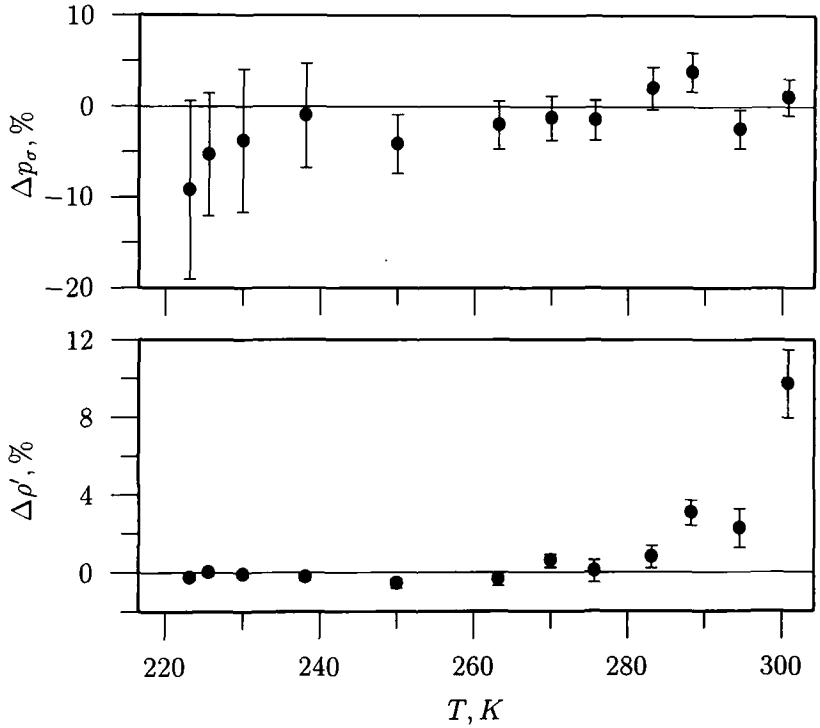

Fig. 1. Deviation plots from EOS [25] for the vapor pressures and bubble densities of carbon dioxide as obtained from simulation (●) with the parameters from Möller and Fischer [10]. The bars indicate the statistical uncertainties. $\Delta p_\sigma = (p_{\sigma,\mathrm{SIM}} - p_{\sigma,\mathrm{EOS}})/p_{\sigma,\mathrm{EOS}}$; $\Delta\rho' = (\rho'_{\mathrm{SIM}} - \rho'_{\mathrm{EOS}})/\rho'_{\mathrm{EOS}}$.

Table II. Simulation Results for the Derivatives of v^E and h^E with Respect to η and ξ as Obtained from Fluctuation Formulae [19] for the Three Mixtures Using the LB Combining Rules: (a) Methane + Ethane at $T = 104$ K, $p = 0$ MPa, and $x_{CH_4} = 0.5$; (b) Methane + Carbon Dioxide at $T = 230$ K, $p = 10$ MPa, and $x_{CH_4} = 0.5$; and (c) Carbon Dioxide + Ethane at $T = 248.1$ K, $p = 3$ MPa, and $x_{CO_2} = 0.5078$

Mixture	$\partial v^E/\partial\eta$ ($cm^3 \cdot mol^{-1}$)	$\partial v^E/\partial\xi$ ($cm^3 \cdot mol^{-1}$)	$\partial h^E/\partial\eta$ ($J \cdot mol^{-1}$)	$\partial h^E/\partial\xi$ ($J \cdot mol^{-1}$)
$CH_4 + C_2H_6$	56.5 (44)[a]	−4.39 (54)	900 (1,100)	−7,060 (190)
$CH_4 + CO_2$	62.1 (93)	−38.1 (45)	−450 (730)	−9,380 (160)
$CO_2 + C_2H_6$	72.8 (86)	−25.3 (29)	−900 (1,800)	−10,400 (1,600)

[a] Numbers in parentheses denote the statistical uncertainties of the last digits.

components, we can calculate v^E_{LB} and h^E_{LB}. On the basis of these results, the unlike interaction parameters are fitted with

$$v^E_{EXP} = v^E_{LB} + \left(\frac{\partial v^E}{\partial \eta}\right)(\eta - 1) + \left(\frac{\partial v^E}{\partial \xi}\right)(\xi - 1) \tag{19}$$

$$h^E_{EXP} = h^E_{LB} + \left(\frac{\partial h^E}{\partial \eta}\right)(\eta - 1) + \left(\frac{\partial h^E}{\partial \xi}\right)(\xi - 1) \tag{20}$$

to the experimental results.

Table III. (a) Volumes and Enthalpies of the Pure Components Methane and Ethane in Comparison to EOS [23, 24] at $T = 104$ K and $p = 0$ MPa; (b) Excess Volumes and Excess Enthalpies of the LB Mixture and the Final Mixture Model[a] at $T = 104$ K and $p = 0$ MPa in Comparison to Experimental Results [20]

a

x_{CH_4}	v_{SIM} ($cm^3 \cdot mol^{-1}$)	v_{EOS} ($cm^3 \cdot mol^{-1}$)	h^{res}_{SIM} ($kJ \cdot mol^{-1}$)	h^{res}_{EOS} ($kJ \cdot mol^{-1}$)
1.0	37.003 (22)	37.019	−8.4188 (52)	−8.4655
0.0	46.850 (13)	47.210	−17.4367 (62)	−17.4676

b

x_{CH_4}	η	ξ	v^E_{SIM} ($cm^3 \cdot mol^{-1}$)	v^E_{EXP} ($cm^3 \cdot mol^{-1}$)	h^E_{SIM} ($J \cdot mol^{-1}$)	h^E_{EXP} ($J \cdot mol^{-1}$)
0.5	1	1	−0.532 (23)	−0.45	67.4 (81)	74
0.5[a]	1.00140	0.99923	−0.451 (29)	−0.45	75 (12)	74

Table IV. (a) Volumes and Enthalpies of the Pure Components Methane and Carbon Dioxide in Comparison to EOS [23, 25] at $T = 230$ K and $p = 10$ MPa; (b) Excess Volumes and Excess Enthalpies of the LB Mixture and the Final Mixture Model[a] at $T = 230$ K and $p = 10$ MPa in Comparison to Results from EOS [22]

a

x_{CH_4}	v_{SIM} ($cm^3 \cdot mol^{-1}$)	v_{EOS} ($cm^3 \cdot mol^{-1}$)	h^{res}_{SIM} ($kJ \cdot mol^{-1}$)	h^{res}_{EOS} ($kJ \cdot mol^{-1}$)
1.0	103.9 (12)	105.4	−3.421 (41)	−3.487
0.0	38.293 (37)	38.232	−14.946 (16)	−15.105

b

x_{CH_4}	η	ξ	v^E_{SIM} ($cm^3 \cdot mol^{-1}$)	v^E_{EOS} ($cm^3 \cdot mol^{-1}$)	h^E_{SIM} ($J \cdot mol^{-1}$)	h^E_{EOS} ($J \cdot mol^{-1}$)
0.5	1	1	−21.63 (62)	−20.43	377 (36)	795
0.5[a]	0.99220	0.95580	−20.25 (63)	−20.43	796 (36)	795

Table V. (a) Volumes and Enthalpies of the Pure Components Carbon Dioxide and Ethane in Comparison to EOS [24, 25] at $T = 248.1$ K and $p = 3$ MPa; (b) Excess Volumes and Excess Enthalpies of the LB Mixture and the Final Mixture Model[a] at $T = 248.1$ K and $p = 3$ MPa in Comparison to Experimental Results [21]

a

x_{CO_2}	v_{SIM} ($cm^3 \cdot mol^{-1}$)	v_{EOS} ($cm^3 \cdot mol^{-1}$)	h^{res}_{SIM} ($kJ \cdot mol^{-1}$)	h^{res}_{EOS} ($kJ \cdot mol^{-1}$)
1.0	41.565 (76)	41.535	−14.024 (26)	−14.183
0.0	65.70 (12)	65.91	−12.561 (21)	−12.581

b

x_{CO_2}	η	ξ	v^E_{SIM} ($cm^3 \cdot mol^{-1}$)	v^E_{EXP} ($cm^3 \cdot mol^{-1}$)	h^E_{SIM} ($J \cdot mol^{-1}$)	h^E_{EXP} ($J \cdot mol^{-1}$)
0.5078	1	1	1.76 (12)	3.1	957 (28)	1509
0.5078[a]	1.00000	0.94691	3.34 (14)	3.1	1547 (29)	1509

Now we have to choose for each mixture a state point in the liquid phase, where experimental results of v^E and h^E are available. For the mixture methane + ethane we use $T = 104$ K, $p = 0$ MPa, and $x_{CH_4} = 0.5$ [20]; for carbon dioxide + ethane $T = 248.1$ K, $p = 3$ MPa, and $x_{CO_2} = 0.5078$ [21]. In the case of methane + carbon dioxide no reliable measurement was found. Therefore we use the DDMIX equation of state [22] to determine at $T = 230$ K, $p = 10$ MPa, and $x_{CH_4} = 0.5$, the excess values $v^E_{EOS} = 20.43\ cm^3 \cdot mol^{-1}$ and $h^E_{EOS} = 795\ J \cdot mol^{-1}$.

One simulation run for each mixture with the assumed LB mixing rule yields the derivatives compiled in Table II. Together with two runs for the pure substances (cf. Tables IIIa–Va), we can calculate the excess volume and excess enthalpy for each LB mixture. Finally, the η and ξ values are evaluated by Eqs. (19) and (20). As a first test of these models a new mixture run is performed, to check whether the fit to the experimental data was successful. On the basis of the results in Tables IIIb–Vb, we can state, that the mixture excess properties are well described by the models.

4. RESULTS AND DISCUSSION

For each of the considered mixtures methane + ethane, methane + carbon dioxide, and carbon dioxide + ethane VLE data were predicted at three temperatures. The isotherms were chosen in the way that comparison with experimental data for vapor pressure and composition is possible. The raw data for the liquid, Eq. (7), were obtained by molecular dynamics simulations. On the vapor side, in 44 of 81 cases it was not necessary to perform simulation runs, in order to obtain Eq. (12). A simple EOS, virial, or perturbed virial expansion was used instead. This reduced our computational effort significantly. The validity of the EOS for the vapor was tested by simulations; when the difference in the chemical potentials from EOS versus from simulation was within the simulation uncertainties, EOS was used. For the remaining 37 coexistence points, Eq. (12) was evaluated by simulations.

4.1. Methane + Ethane

VLE data are presented for the temperatures 160, 199.93, and 250 K in Table VI. Within its range of validity a perturbed virial expansion-type EOS, the Haar–Shenker–Kohler equation (HSK) [26] in combination with an appropriate hard-sphere mixture equation was used for the vapor. Figure 2a shows a comparison of the present work with EOS [27] and experimental results [28–30] in the pressure-composition diagram. The

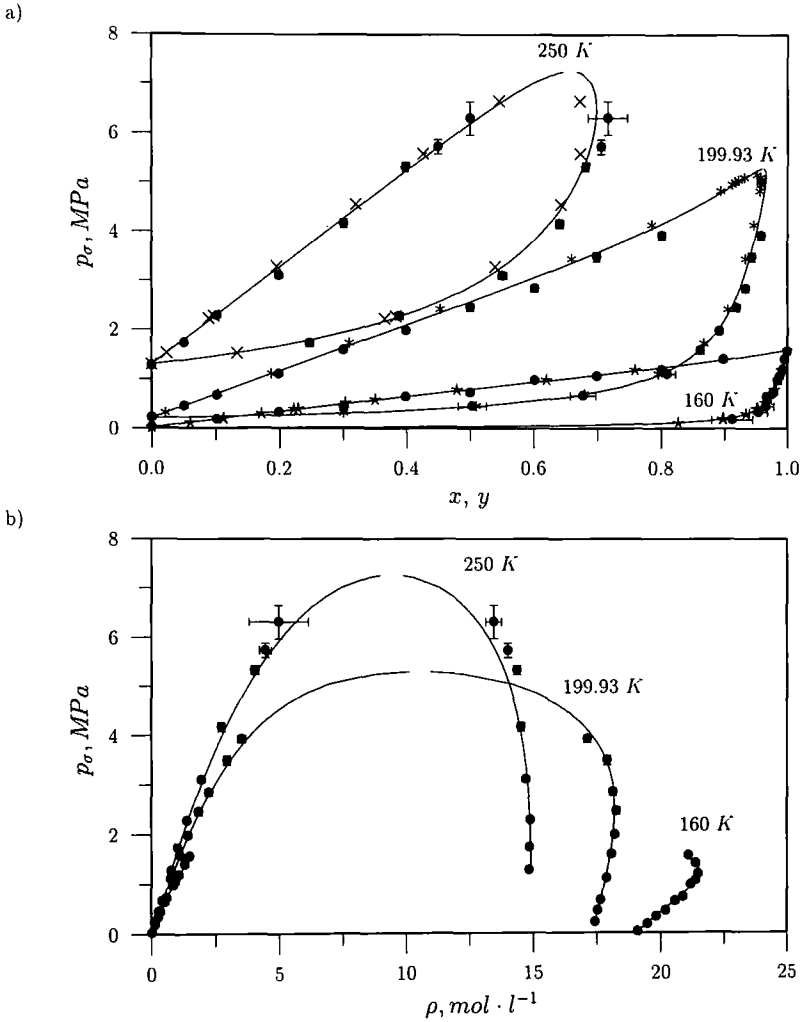

Fig. 2. (a) Vapor pressure vs composition and (b) vapor pressure vs density diagram for the mixture methane + ethane at 160, 199.93, and 250 K. Present results (●) are given in comparison to EOS results of Müller et al. [27] (——). In the pressure vs. composition diagram experimental VLE are shown: Miller et al. [28] at 160 K (★), Wichterle and Kobayashi [29] at 199.93 K (*), and Davalos et al. [30] at 250 K (×).

Table VI. Vapor–Liquid Phase Equilibria of the Mixture Methane + Ethane as Calculated by the NpT + Test Particle Method[a]

x_{CH_4}	y_{CH_4}	p_σ (MPa)	ρ' (mol · l^{-1})	ρ'' (mol · l^{-1})	h'^{res} (kJ · mol^{-1})	h''^{res} (kJ · mol^{-1})
			$T = 160.00$ K			
0.00000	0.00000	0.0218(64)	19.122(10)	0.0167(48)	−15.5738(93)	−0.040 (11)
0.10156	0.912 (33)	0.180 (15)	19.482(13)	0.139 (12)	−14.679 (11)	−0.0887(93)
0.19922	0.954 (15)	0.330 (26)	19.831(18)	0.259 (21)	−13.817 (13)	−0.152 (13)
0.30078	0.966 (13)	0.448 (35)	20.201(18)	0.356 (30)	−12.953 (12)	−0.205 (18)
0.39844	0.9671 (62)	0.642 (44)	20.576(18)	0.525 (40)	−12.122 (12)	−0.301 (23)
0.50000	0.9780 (27)	0.726 (39)	20.888(18)	0.600 (36)	−11.2544(96)	−0.336 (20)
0.60156	0.9845 (19)	0.975 (47)	21.171(25)	0.837 (47)	−10.375 (12)	−0.461 (26)
0.69922	0.98789(76)	1.058 (43)	21.368(30)	0.920 (44)	−9.532 (13)	−0.503 (24)
0.80078	0.99252(72)	1.191 (50)	21.463(31)	1.058 (54)	−8.650 (12)	−0.573 (29)
0.89844	0.99577(23)	1.404 (54)	21.370(48)	1.296 (64)	−7.788 (15)	−0.696 (34)
1.00000	1.00000	1.562 (25)	21.086(26)	1.483 (32)	−6.9027(76)	−0.793 (20)
			$T = 199.93$ K			
0.00000	0.00000	0.218 (17)	17.423(19)	0.138 (11)	−14.279 (16)	−0.253 (21)
0.05078	0.503 (22)	0.450 (21)	17.537(21)	0.288 (14)	−13.828 (17)	−0.294 (17)
0.10156	0.677 (20)	0.663 (27)	17.649(23)	0.429 (19)	−13.393 (18)	−0.342 (18)
0.19922	0.810 (13)	1.103 (36)	17.874(23)	0.736 (27)	−12.569 (15)	−0.476 (20)
0.30078	0.8622 (61)	1.586 (48)	18.069(27)	1.100 (39)	−11.693 (17)	−0.650 (24)
0.39844	0.8915 (42)	1.982 (48)	18.198(32)	1.424 (42)	−10.865 (17)	−0.798 (24)
0.50000	0.9189 (33)	2.458 (75)	18.265(38)	1.843 (73)	−9.993 (18)	−0.980 (39)
0.60156	0.9332 (17)	2.846 (71)	18.110(43)	2.221 (76)	−9.065 (19)	−1.146 (38)
0.69922*	0.9437 (14)	3.490 (94)	17.891(66)	2.95 (13)	−8.190 (24)	−1.461 (66)
0.80078*	0.95792(98)	3.924 (78)	17.119(92)	3.53 (17)	−7.173 (27)	−1.684 (84)
			$T = 250.00$ K			
0.00000	0.00000	1.271 (32)	14.815(34)	0.746 (24)	−12.372 (20)	−1.105 (36)
0.05078	0.2475 (58)	1.726 (38)	14.845(38)	1.017 (30)	−11.944 (26)	−1.156 (34)
0.10156	0.3879 (67)	2.279 (41)	14.879(39)	1.387 (36)	−11.541 (27)	−1.339 (36)
0.19922*	0.5514 (68)	3.104 (53)	14.686(62)	1.936 (47)	−10.596 (35)	−1.478 (51)
0.30078*	0.6406 (62)	4.166 (88)	14.507(65)	2.74 (11)	−9.661 (34)	−1.820 (78)
0.39844*	0.6819 (47)	5.321 (91)	14.343(75)	4.04 (15)	−8.840 (34)	−2.509 (98)
0.44922*	0.7057 (52)	5.73 (15)	13.997(96)	4.45 (23)	−8.296 (39)	−2.64 (13)
0.50000*	0.716 (31)	6.31 (34)	13.44 (31)	5.0 (12)	−7.68 (11)	−2.83 (67)

[a] For the vapor phase, the HSK equation [26] was always used, except for the state points indicated by a superscript asterisk. The residual enthalpy is given as $h^{res} = h(T, p, x) - h(T, 0, x)$.

pressure–density diagram (Fig. 2b) gives a comparison between the present work and the EOS. Remember that the fit of the unlike interaction parameters was made with an experimental pair of v^E and h^E at $T = 104$ K, which is well below the temperature range where VLE data are calculated.

From Fig. 2a we learn that at 160 K the experimental data are met within the uncertainties of the simulation. For low compositions of methane in the liquid, the calculated vapor compositions show some uncertainties caused by the flat slope of the dew line. At the medium temperature the vapor pressure of the VLE points for $x_{CH_4} \geqslant 0.4$ are somewhat too low. Their

Table VII. Vapor–Liquid Phase Equilibria of the Mixture Methane + Carbon Dioxide as Calculated by the NpT + Test Particle Method[a]

x_{CH_4}	y_{CH_4}	p_σ (MPa)	ρ' (mol · l^{-1})	ρ'' (mol · l^{-1})	h'^{res} (kJ · mol^{-1})	h''^{res} (kJ · mol^{-1})
			$T = 230.00$ K			
0.00000	0.00000	0.859(71)	25.605(30)	0.497(46)	−15.002(19)	−0.568(52)
0.02344*	0.358 (18)	1.307(20)	25.264(36)	0.839(47)	−14.573(21)	−0.73 (11)
0.05078*	0.517 (16)	2.014(66)	25.004(46)	1.227(53)	−14.163(26)	−0.792(48)
0.10156*	0.677 (19)	3.03 (17)	24.536(47)	1.91 (12)	−13.433(24)	−1.054(73)
0.14844*	0.712 (11)	3.73 (11)	23.950(54)	2.51 (13)	−12.760(29)	−1.340(84)
0.19922*	0.7437 (95)	4.43 (20)	23.338(62)	3.10 (24)	−12.047(29)	−1.53 (13)
0.25000*	0.7550 (70)	4.99 (17)	22.675(69)	3.72 (23)	−11.338(29)	−1.83 (12)
0.30078*	0.7572 (82)	5.92 (25)	22.170(81)	4.95 (40)	−10.708(26)	−2.38 (20)
			$T = 250.00$ K			
0.00000	0.00000	1.712(58)	23.627(56)	0.977(40)	−13.837(31)	−1.018(42)
0.02344*	0.2224 (75)	2.49 (11)	23.550(51)	1.456(58)	−13.545(28)	−1.187(33)
0.05078*	0.358 (12)	3.110(85)	23.133(64)	1.884(79)	−13.082(30)	−1.333(78)
0.10156*	0.493 (10)	4.03 (13)	22.459(63)	2.53 (11)	−12.333(29)	−1.606(88)
0.14844*	0.5550 (71)	4.94 (13)	21.802(71)	3.28 (13)	−11.649(33)	−1.873(69)
0.19922*	0.5905 (75)	5.79 (15)	21.151(75)	4.13 (20)	−10.967(33)	−2.27 (13)
0.25000*	0.6145 (63)	6.24 (23)	20.12 (11)	4.55 (27)	−10.221(41)	−2.38 (14)
0.30078*	0.6276 (82)	6.94 (19)	19.33 (12)	5.56 (36)	−9.550(40)	−2.83 (18)
			$T = 270.00$ K			
0.00000	0.00000	3.163(78)	21.630(73)	1.901(72)	−12.695(35)	−1.829(70)
0.02344*	0.1307 (38)	3.922(93)	21.284(83)	2.380(83)	−12.301(39)	−1.958(77)
0.05078*	0.2307 (75)	4.63 (16)	20.96 (13)	2.87 (14)	−11.910(56)	−2.12 (11)
0.10156*	0.3489 (53)	5.66 (11)	20.010(80)	3.63 (11)	−11.059(33)	−2.319(75)
0.14844*	0.4067 (59)	6.58 (19)	19.09 (13)	4.35 (19)	−10.307(46)	−2.57 (11)
0.19922*	0.4366 (91)	7.79 (35)	18.49 (18)	5.88 (45)	−9.698(61)	−3.33 (21)

[a] For the vapor phase, the second virial coefficients were always used, exept for the state points indicated by a superscript asterisk. The residual enthalpy is given as $h^{res} = h(T, p, x) - h(T, 0, x)$.

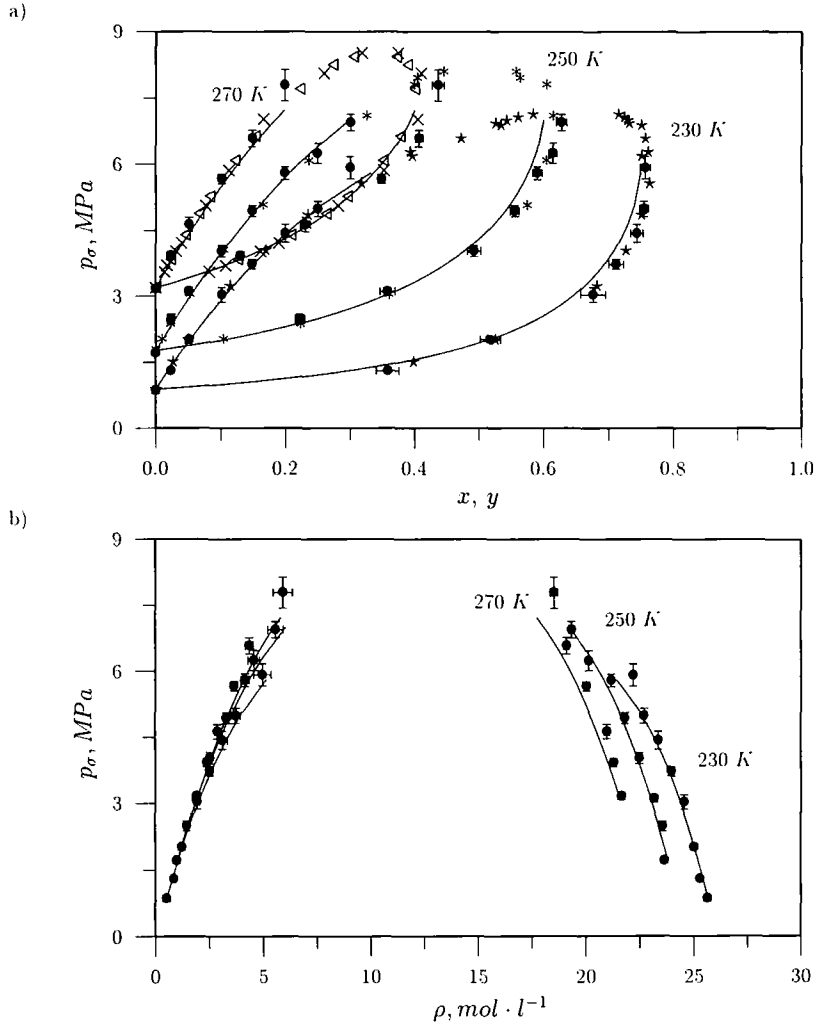

Fig. 3. (a) Vapor pressure vs composition and (b) vapor pressure vs density diagram for the mixture methane + carbon dioxide at 230, 250, and 270 K. Present results (●) are given in comparison to EOS results of Ely et al. [22] (——). In the pressure vs composition diagram experimental VLE are shown: Davalos et al. [30] at 230 K (★), at 250 K (∗), and at 270 K (×) and Somait and Kidnay [31] at 270 K (◁).

deviation from experimental and EOS results is outside of the calculated error bars. The vapor compositions in the upper part of the isotherm $T = 250$ K are systematically somewhat too high. The highest VLE point has the largest statistical uncertainties, which is caused by its vincinity to the critical point.

Regarding Fig. 2b, we can observe for the low temperature a perfect agreement between simulation and EOS data. At the medium temperature the present results follow the EOS line very well; the vapor pressure of the highest point seems to be too low. For 250 K the simulation densities at high pressure show some deviation from EOS results, which reflects the tendency of simulation to yield a too high critical temperature.

4.2. Methane + Carbon Dioxide

VLE data are presented for the temperatures 230, 250, and 270 K in Table VII. The raw data for the vapor in the mixture were always obtained by simulation. Figure 3a shows a comparison of the present work with EOS [22] and experimental results [30, 31] in the pressure–composition diagram. The pressure–density diagram (Fig. 3b) gives a comparison between the present work and the EOS.

In Fig. 3a it is remarkable that, for the lower two temperatures, our results are much closer to the experimental data than the EOS. This is somewhat surprising, because we did not use experimental data to fit the mixture model, but the EOS. At the high temperature this holds for the bubble line, whereas the vapor compositions from simulation are slightly too high.

Regarding Fig. 3b where all three temperatures considered are well above the critical temperature of methane, we can observe again the tendency of simulation to yield a too high critical temperature. For 230 and 250 K the present results on the bubble line agree within their error bars with the EOS, except the highest point at 230 K. For 270 K most of our points are outside of their uncertainties higher than the EOS results. But keeping in mind the significant differences between EOS and experimental data in Fig. 3a, the performance of the EOS here is questionable.

4.3. Carbon Dioxide + Ethane

VLE data are presented for the temperatures 223.15, 250, and 283.15 K in Table VIII. Within its range of validity a virial expansion truncated after the second coefficient was used for the vapor. Figure 4a shows a comparison of the present work with EOS [22] and experimental results [32, 30] in the pressure–composition diagram. The pressure–density

Table VIII. Vapor–Liquid Phase Equilibria of the Mixture Carbon Dioxide + Ethane as Calculated by the NpT + Test Particle Method[a]

x_{CO_2}	y_{CO_2}	p_σ (MPa)	ρ' (mol·l^{-1})	ρ'' (mol·l^{-1})	h'^{res} (kJ·mol^{-1})	h''^{res} (kJ·mol^{-1})
			$T = 223.15$ K			
0.00000	0.00000	0.570(24)	16.337(18)	0.343(16)	−13.472(14)	−0.562(26)
0.10156	0.2654 (79)	0.680(20)	16.721(26)	0.409(14)	−13.131(20)	−0.573(19)
0.19922	0.387 (10)	0.804(22)	17.213(33)	0.491(16)	−12.929(23)	−0.647(21)
0.39844	0.523 (11)	0.908(22)	18.512(27)	0.560(16)	−12.845(18)	−0.700(20)
0.60156	0.630 (10)	0.895(21)	20.255(30)	0.547(15)	−13.128(22)	−0.663(18)
0.80078	0.700 (15)	0.918(38)	22.722(36)	0.562(27)	−13.908(21)	−0.670(32)
0.89844	0.755 (14)	0.851(33)	24.254(36)	0.514(23)	−14.520(25)	−0.608(27)
1.00000	1.00000	0.620(67)	26.152(30)	0.361(42)	−15.353(19)	−0.428(50)
			$T = 250.00$ K			
0.00000	0.00000	1.266(30)	14.856(36)	0.742(23)	−12.399(27)	−1.100(33)
0.10156	0.2226 (42)	1.592(30)	15.221(36)	0.958(25)	−12.093(25)	−1.241(33)
0.19922	0.3514 (56)	1.765(32)	15.561(40)	1.074(27)	−11.827(26)	−1.299(33)
0.30078	0.4476 (70)	1.931(40)	15.961(58)	1.193(35)	−11.629(35)	−1.381(41)
0.39844	0.5165 (59)	2.077(32)	16.598(45)	1.306(30)	−11.612(28)	−1.471(33)
0.50000	0.5846 (65)	2.077(35)	17.210(48)	1.290(31)	−11.626(27)	−1.419(35)
0.60156	0.6368 (67)	2.160(42)	18.088(56)	1.353(38)	−11.775(33)	−1.465(41)
0.69922	0.6877 (67)	2.190(47)	19.158(61)	1.370(42)	−12.100(35)	−1.465(45)
0.80078	0.7566 (70)	2.110(49)	20.366(58)	1.291(42)	−12.510(30)	−1.362(44)
0.89844	0.8426 (53)	1.988(51)	21.790(52)	1.185(40)	−13.049(27)	−1.236(42)
1.00000	1.00000	1.712(58)	23.627(56)	0.977(40)	−13.837(31)	−1.018(42)
			$T = 283.15$ K			
0.00000*	0.00000	3.008(58)	12.489(75)	1.896(67)	−10.716(47)	−2.394(81)
0.10156*	0.1717 (28)	3.594(60)	12.667(61)	2.298(61)	−10.351(38)	−2.559(66)
0.19922*	0.2908 (36)	4.029(51)	12.822(77)	2.778(84)	−10.039(43)	−2.929(83)
0.30078*	0.3949 (49)	4.259(85)	12.88 (12)	2.96 (13)	−9.686(63)	−2.96 (12)
0.39844*	0.4749 (37)	4.653(53)	13.05 (13)	3.36 (11)	−9.467(64)	−3.191(89)
0.50000*	0.5587 (46)	4.790(79)	13.18 (13)	3.42 (17)	−9.264(68)	−3.13 (14)
0.60156*	0.6394 (36)	4.901(67)	13.84 (15)	3.45 (13)	−9.391(70)	−3.11 (10)
0.69922*	0.7083 (39)	5.017(97)	14.61 (25)	3.56 (14)	−9.60 (11)	−3.18 (12)
0.80078*	0.7892 (34)	5.01 (12)	16.38 (14)	3.45 (16)	−10.288(64)	−2.99 (13)
0.89844*	0.8769 (21)	4.897(74)	17.72 (10)	3.22 (12)	−10.827(46)	−2.78 (11)
1.00000*	1.00000	4.59 (11)	19.73 (11)	2.82 (11)	−11.659(51)	−2.43 (10)

[a] For the vapor phase the second virial coefficients were always used, exept for the state points indicated by a superscript asterisk. The residual enthalpy is given as $h^{res} = h(T, p, x) - h(T, 0, x)$.

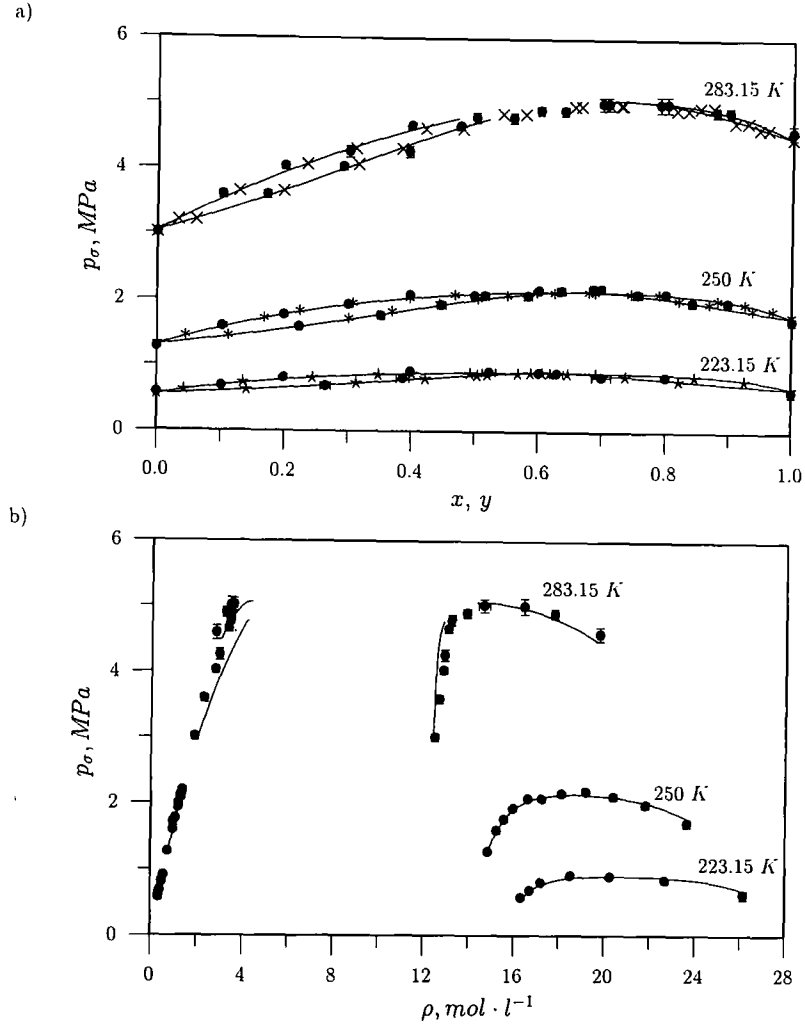

Fig. 4. (a) Vapor pressure vs composition and (b) vapor pressure vs density diagram for the mixture carbon dioxide + ethane at 223.15, 250, and 283.15 K. Present results (●) are given in comparison to EOS results of Ely et al. [22] (——). In the pressure vs composition diagram experimental VLE are shown: Fredenslund and Mollerup. [32] at 223.15 K (★), Davalos et al. [30] at 250 K (∗), and Fredenslund and Mollerup [32] at 283.15 K (×).

diagram (Fig. 4b) gives a comparison between the present work and the EOS. It should be mentioned that the system considered here shows a well-known azetropic behavior.

By inspection of Fig. 4a we observe for all three temperatures an excellent agreement among the simulation, experimental, and EOS data. At the highest temperature the EOS, namely the DDMIX code, did not yield reliable results in a certain composition range.

In Fig. 4b we can see an unusual shape of the isotherms. For the two lower temperatures the agreement between simulation and EOS is very good, whereas for the high temperature systematic deviations can be seen. Regarding the fact that the EOS did not yield the complete isotherm, it is questionable which results are better.

5. SUMMARY

It can be stated that we have constructed models of three technically important mixtures. This was done on the basis of molecular models for the pure substances, and with the help of some few experimental mixture data, namely, one pair of v^E and h^E for each mixture. It was found that these models yield very accurate predictions of the mixture phase equilibria. A crucial item in the whole procedure, however, is the pure substance models. Deficiencies of these models have a strong impact on the mixture properties which cannot be remedied by the unlike interaction parameters.

APPENDIX

This Appendix summarizes some details of our molecular dynamics simulations. All runs were performed in the NpT ensemble with 256 particles. Periodic boundary conditions and the minimum image convention were used, with a cutoff radius of 3.5σ, where σ is the size parameter of the lower boiling substance; the long-range corrections were considered. In the case of quadrupolar interactions, no long-range corrections had to be made. The translational equations of motion were solved with a fifth-order predictor–corrector method. The time step was taken to be 0.0015 in the usual units. Each run was started from a fcc-lattice with 5000 equilibration time steps; its production length was 60,000 time steps. The pressure was kept constant by the method of Andersen [33], where the membrane mass was set to 10^{-6} in the vapor and 5×10^{-4} in the liquid at low temperatures; the temperature was kept constant by momentum scaling after each time step. In order to calculate the chemical potentials and the partial molar volumes, Widom's test particle insertion was applied, using 512 or 1024 test particles for the liquid and 256 for the vapor after each time step. Inserting

quadrupolar particles, their potential energy ψ was set to infinity in the case of distances smaller than 0.4σ [10]. The uncertainties of the results were calculated according to the method of Fincham et al. [34].

ACKNOWLEDGMENTS

The authors thank Professor J. Ely (Golden, Colorado) for having made available to them the program package DDMIX. They also thank Dr.-Ing. M. Wendland (Wien) for helpful discussions. The simulation runs were performed on the Siemens S600 computer at the Rechenzentrum der RWTH Aachen. This work was supported by Deutsche Forschungsgemeinschaft (DFG) Az Fi 287/11-1.

REFERENCES

1. A. Z. Panagiotopoulos, *Mol. Phys.* **61**:813 (1987).
2. K. E. Gubbins, *Mol. Simulat.* **2**:223 (1989).
3. A. Z. Panagiotopoulos, *Int. J. Thermophys.* **10**:447 (1989).
4. A. Z. Panagiotopoulos, *Mol. Simulat.* **9**:1 (1992).
5. B. Smit, in M. P. Allen, and D. J. Tildesley, eds., *Computer Simulation in Chemical Physics* (Kluwer, Dordrecht, 1993), pp. 173–209.
6. D. Möller and J. Fischer, *Mol. Phys.* **69**:463 (1990), **75**:1461 (1992).
7. A. Lotfi, J. Vrabec, and J. Fischer, *Mol. Phys.* **76**:1319 (1992).
8. C. Kriebel, A. Müller, J. Winkelmann, and J. Fischer, *Mol. Phys.* **84**:381 (1995).
9. D. Boda, J. Liszi, and I. Szalai, *Chem. Phys. Lett.* **235**:140 (1995).
10. D. Möller and J. Fischer, *Fluid Phase Equil.* **100**:35 (1994).
11. J. Vrabec and J. Fischer, *Mol. Phys.* **85**:781 (1995).
12. J. Vrabec, A. Lotfi, and J. Fischer, *Fluid Phase Equil.* **112**:173 (1995).
13. A. Lotfi, Dr.-Ing. thesis (Ruhr-Universtät, Bochum). See also *Fortschrittberichte VDI, Reihe* 3, *Nr.* 335 (VDI-Verlag, Düsseldorf, 1993).
14. J. Vrabec, D. Möller, C. Kriebel, A. Müller, C. J. Wormald, and J. Fischer, manuscript in preparation (1996).
15. D. Möller, J. Oprzynski, A. Müller, and J. Fischer, *Mol. Phys.* **75**:363 (1992).
16. B. Widom, *J. Chem. Phys.* **39**:2808 (1963).
17. P. Sindzingre, G. Ciccotti, C. Massobrio, and D. Frenkel, *Chem Phys. Lett.* **136**:35 (1987).
18. D. M. Heyes, *Mol. Simulat.* **8**:227 (1992).
19. J. Fischer, D. Möller, A. Chialvo, and J. M. Haile, *Fluid Phase Equil.* **48**:161 (1989).
20. J. C. G. Calado, E. J. S. Gomes de Azevedo, and V. A. M. Soares, *Chem. Eng. Comm.* **5**:149 (1980).
21. C. J. Wormald and J. M. Eyears, *J. Chem. Thermodynam.* **20**:323 (1988).
22. J. F. Ely, J. W. Magee and W. M. Haynes, *NBS Standard Reference Database* 14, DDMIX, Version 9.06 (NIST, Boulder, CO, 1989).
23. U. Setzmann and W. Wagner, *J. Phys. Chem. Ref. Data* **20**:1061 (1991).
24. D. G. Friend, H. Ingham, and J. F. Ely, *J. Phys. Chem. Ref. Data* **20**:275 (1991).
25. R. Span and W. Wagner, *J. Phys. Chem. Ref. Data*, in press (1996).
26. J. Fischer and M. Bohn, *Mol. Phys.* **58**:395 (1986).
27. A. Müller, J. Winkelmann, and J. Fischer, submitted for publication (1996).
28. R. C. Miller, A. J. Kidnay, and M. J. Hiza, *J. Chem. Thermodynam.* **9**:167 (1977).

29. I. Wichterle and R. Kobayashi, *J. Chem. Eng. Data* **17**:9 (1972).
30. J. Davalos, W. R. Anderson, R. E. Phelps, and A. J. Kidnay, *J. Chem. Eng. Data* **21**:81 (1976).
31. F. A. Somait and A. J. Kidnay, *J. Chem. Eng. Data* **23**:301 (1978).
32. A. Fredenslund and J. Mollerup, *J. Chem. Soc. Faraday Trans. I* **70**:1653 (1974).
33. H. C. Andersen, *J. Chem. Phys.* **72**:2384 (1980).
34. D. Fincham, N. Quirke, and D. J. Tildesley, *J. Chem. Phys.* **84**:4535 (1986).